

Andreev-Like Reflections with Cold Atoms

A. J. Daley,^{1,2} P. Zoller,^{1,2} and B. Trauzettel^{3,4}¹*Institute for Quantum Optics and Quantum Information, Austrian Academy of Sciences, A-6020 Innsbruck, Austria*²*Institute for Theoretical Physics, University of Innsbruck, A-6020 Innsbruck, Austria*³*Department of Physics and Astronomy, University of Basel, Basel, Switzerland*⁴*Institute for Theoretical Physics, University of Würzburg, D-97074 Würzburg, Germany*

(Received 14 October 2007; published 20 March 2008)

We propose a setup in which Andreev-like reflections predicted for 1D transport systems could be observed time dependently using cold atoms in a 1D optical lattice. Using time-dependent density matrix renormalization group methods we analyze the wave packet dynamics as a density excitation propagates across a boundary in the interaction strength. These phenomena exhibit good correspondence with predictions from Luttinger liquid models and could be observed in current experiments in the context of the Bose-Hubbard model.

DOI: 10.1103/PhysRevLett.100.110404

PACS numbers: 03.75.Lm, 42.50.-p, 72.10.-d

The rich physics described by Luttinger liquid (LL) theory [1] is normally associated with interacting one-dimensional (1D) electron systems such as carbon nanotubes or lithographically defined quantum wires. However, exciting progress in cold atomic gases experiments [2,3] has seen aspects of this physics realized in a new context [4,5]. This not only promises observation of effects such as spin-charge separation [5] in a clean system closely realizing the theoretical models, but also provides a new viewpoint on transport properties, which can be studied in the context of coherent wave packet propagation. This connection is strengthened by the use of recently developed time-dependent density matrix renormalization group (TDMRG) methods [6], which allow the computation of dynamics for physically realizable lattice models, and the identification of parameter ranges in which LL model predictions can be observed in experiments. Here we investigate this analogy for systems described by the inhomogeneous LL model, in which the electron-electron interaction varies stepwise from essentially noninteracting to repulsively interacting [7]. This model is used to describe the coupling of quantum wires to higher dimensional leads which act as weakly interacting electron reservoirs, and predicts rich boundary phenomena, including Andreev-like reflection, i.e., reflection of hole excitations. We show that analogous Andreev-like reflections can exist for 1D atomic gases in optical lattices, where the many-body dynamics are well described by Hubbard models [8], and that these could be observed time dependently in current experimental setups.

Andreev-like reflections are predicted by an inhomogeneous LL model with Hamiltonian [7] ($\hbar = 1$) $H_{LL} = \int (dx/2\pi) [u(x)g(x)(\pi\Pi)^2 + u(x)(\partial_x\Phi)^2/g(x)]$, where Φ is the standard Bose field operator in bosonization [1], and Π its conjugate momentum density, $[\Pi(x), \phi(x')] = i\delta(x - x')$. This model describes low energy excitations with speed of sound $u(x)$. The parameter $g(x)$ characterizes interactions, with $0 < g(x) < 1$ for repulsive interactions,

$g(x) = 1$ in the noninteracting case, and $g(x) > 1$ for attractive interactions. When a propagating density excitation is incident on a boundary at x_B with $g(x < x_B) = g_L$ and $g(x \geq x_B) = g_R$, the strength of the reflections is quantified by a reflection coefficient $\gamma = (g_L - g_R)/(g_L + g_R)$ [see Fig. 1(b)]. For $\gamma < 0$, excitations are transmitted with a larger amplitude $1 - \gamma$, which is compensated by the reflection of holelike charge excitations with amplitude $|\gamma|$ [see Fig. 1(a), bottom]. This is analogous to Andreev reflection when an electron is incident on a normal metal-superconductor boundary: The electron forms a Cooper pair in the superconductor, and depending on whether its energy is higher or lower than the superconducting gap, a partial or complete hole is reflected.

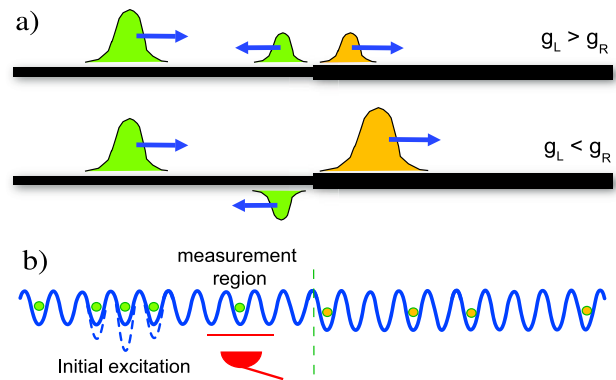


FIG. 1 (color online). (a) A propagating excitation exhibits normal reflections (top) or Andreev reflections (bottom) at an interaction boundary depending on the relative interaction strengths on the two sides. (b) Observation via bosons in an optical lattice in three steps: Preparation of the initial excitation using a superimposed trap (left); propagation of the excitation towards the interaction boundary, formed by coupling the atoms off resonantly to an additional internal state (right); and detection via measurement of the atom density in a region between the initial excitation and the interaction boundary.

Here there is no gap, and so the holes reflected are partial holes [7]. This phenomenon is manifest in several effects predicted for transport through quantum wires—such as oscillations of the nonlinear current voltage characteristics and the appearance of fractional charge excitations in the finite frequency current noise [9]. However, imperfections including contact resistance between quantum wires and the attached electron reservoirs have so far prevented these effects from being observed. In this sense, cold atoms in optical lattices would constitute an ideal physical system in which Andreev-like reflections can be observed.

We study dynamics on the lattice because the physics of atoms in optical lattices is well understood on a microscopic level [8], and TDMRG methods allow exact computation of the dynamics. We first investigate an extended Hubbard model with off-site interactions for spin-polarized fermions (or hard-core bosons), which corresponds in the continuum limit to a Luttinger liquid [1]. The Hamiltonian is given by ($\hbar = 1$)

$$\hat{H} = -J \sum_{\langle i,j \rangle} \hat{c}_i^\dagger \hat{c}_j + \sum_i V_i \hat{n}_i \hat{n}_{i+1} + \sum_i \varepsilon_i \hat{n}_i, \quad (1)$$

where \hat{c}_i annihilates a fermion (or boson) on site i , J is the tunneling rate between neighboring sites, $n_i = \hat{c}_i^\dagger \hat{c}_i$ is the number operator for particles on site i , V_i is the nearest neighbor interaction energy, and ε_i denotes the energy offset of site i due to external potentials. This Hamiltonian is valid for $J, V_i \bar{n} \ll \omega$ with \bar{n} the mean density, and ω the band separation. In the limit $aV_i/v_F \gtrsim 1$, where v_F is the Fermi velocity and a the lattice spacing, the connection between LL physics and this model is approximately given by $g_i = 1/\sqrt{1 + aV_i/v_F}$.

Off-site interactions can be generated with Fermions, e.g., using polar molecules or by coupling to Rydberg states, or with hard-core bosons by loading strongly interacting atoms into excited Bloch bands [10]. However, the natural experimental situation is to have short-range contact interactions between atoms, as described by the Bose-Hubbard model including only on-site interactions, with Hamiltonian ($\hbar = 1$)

$$\hat{H} = -J \sum_{\langle i,j \rangle} \hat{b}_i^\dagger \hat{b}_j + \sum_i U_i \hat{n}_i (\hat{n}_i - 1) + \sum_i \varepsilon_i \hat{n}_i. \quad (2)$$

Analogously to Eq. (1), \hat{b}_i annihilates a boson on site i , $n_i = \hat{b}_i^\dagger \hat{b}_i$, and U_i denotes the on-site interaction energy shift between two atoms. This Hamiltonian is valid in the limit where $J, U_i \bar{n} \ll \omega$. Note that in the limit $|U_i/J|, |U_i/\varepsilon_i| \gg 1$ and with a mean filling factor $\bar{n} \ll 1$ we can obtain the off-site interactions of the extended Hubbard Hamiltonian, Eq. (1), directly from on-site interactions. Restricting to the manifold of states containing only singly occupied sites, we obtain off-site interactions in perturbation theory as $V_{i,\text{eff}} = -J^2/U_i - J^2/U_{i+1}$. Below we go beyond this limit in our numerical calculations.

We begin by studying dynamics in the extended Hubbard model, Eq. (1), before returning to the Bose-Hubbard model below. We consider an initial density excitation formed by a local dip in the external potential [e.g., from a focused laser beam, see Fig. 1(b)],

$$\varepsilon_i = -\theta(-t)\varepsilon_0 \exp[-(i - x_0)^2/(2\sigma^2)] + \varepsilon_R F(i). \quad (3)$$

We compute the ground state of the Hamiltonian (1), and then at $t = 0$, we switch off the local dip suddenly, leaving a Gaussian shaped density excitation centered on site x_0 with width σ and amplitude controlled by ε_0 . The last term denotes the change in potential at the barrier, with $F(x)$ varying linearly across the width of the barrier (M_b sites), $F(i) = 0, i < x_b$; $F(i) = (i - x_b)/M_b, x_b \leq i \leq x_b + M_b$; $F(i) = 1, i > x_b + M_b$. The interaction V_i also varies as $V_i = V_L + (V_R - V_L)F(i)$, and initially we will consider a sharp barrier, $M_b = 1$. The parameter ε_R should be adjusted so that the density on each side of the barrier is approximately the same. Note that this is only possible in the range $|V_L - V_R| \lesssim J$, as otherwise large density oscillations are observed near the boundary. The initial ground state and propagation are computed by quasiexact imaginary and real time evolution, respectively, with Hamiltonian (1), using TDMRG methods [6], which provide an adaptive decimation of the Hilbert space. We performed convergence tests to ensure the accuracy of our results (see [11] for a general analysis of the accuracy of these methods), and estimate errors smaller than a few percent in the presented values.

In Figs. 2(a) and 2(b) we show shaded plots of the atom density at each site varying with time. The initial density excitation splits into right- and left-moving excitations, with the right-moving excitation giving rise to reflected and transmitted excitations after incidence on the boundary. Figure 2(a), for which $V_L = 0$ and $V_R = J$, shows normal reflection of the excitation, where two lower density excitations are produced. In Fig. 2(b), where $V_R = -J$, an Andreev-like reflection is observed, with a hole excitation reflected that corresponds to a lower density at the sites it occupies. Commensurately, a larger amplitude excitation is transmitted at the interaction boundary.

We can quantify this process by defining the amplitude of a density excitation to be the total integrated change from the background density over the sites containing the excitation. The reflection coefficient R naturally follows as the ratio of amplitudes of the reflected and incident excitations. In practice, we identify a group of sites between the original location of the density excitation and the interaction boundary as the measurement region. As shown in Fig. 2(c), the density in the measurement region increases and then decreases as the initial right-moving excitation passes, then we observe either an increase or decrease in the density resulting from normal or Andreev-like reflections, respectively. We then compute R as the ratio of the peak values in each of these time periods. Note

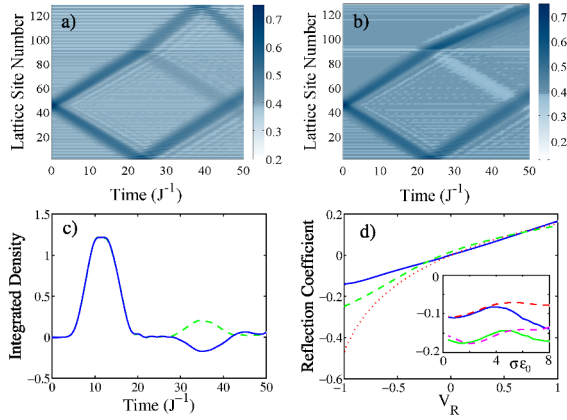


FIG. 2 (color online). Numerical simulation results for propagation of an initial density excitation ($\varepsilon_0 = 2J$, $\sigma = 3$, $x_0 = 45$) across an interaction boundary from $V_L = 0$ to varying V_R at $x_b = 90$ ($M_b = 1$), with open boundary conditions. (a) Shaded density plot for $V_R = J$, showing a normal (positive density) reflection at the boundary. (b) Shaded density plot for $V_R = -J$, showing an Andreev (negative density, or hole) reflection at the boundary. (c) Difference from the initial value of the integrated density over sites 60–75, showing an initial peak due to propagation of the initial density excitation, and a secondary maximum ($V_R = J$, dashed line) or minimum ($V_R = -J$, solid line) due to the reflected excitation. (d) Reflection coefficients as a function of V_R , showing the comparison between simulation values (solid line) and estimated parameters from LL theory using numerically computed Luttinger parameters [from Eq. (4), dashed line] and the analytical form $g = 1/\sqrt{1 + aV_i/v_F}$ (dotted line). The inset shows the dependence on the depth ε_0 with $\sigma = 2$ (solid lines) and $\sigma = 4$ (dashed lines) for $V_R = -0.5J$ (upper curves) and $V_R = -J$ (lower curves), computed from measurement sites 50–70.

that this definition can be used operationally in an experiment, where the integrated density over several sites can be measured, e.g., using fluorescence or phase-contrast imaging with a focused laser [see Fig. 1(b)].

In Fig. 2(d) we plot the reflection coefficient R for $-J < V_R < J$, choosing $V_L = 0$, $\varepsilon_0 = 2J$, and $\sigma = 3$, and see clearly the crossover from Andreev to normal reflection. The quantitative values, though not the variation with V_R , are dependent on the size of the initial excitation, as shown in the inset of Fig. 2(d). In order to compare our results with the known analytical result from LL theory, we extracted approximate Luttinger parameters g_{eff} for the ground states of our extended Hubbard model, Eq. (1), at the background density value for each V_R . This was done by computing density-density correlations and fitting the standard form for these in a LL [1],

$$\langle \hat{n}_0 \hat{n}_r \rangle \approx -\frac{g_{\text{eff}}}{2\pi^2 r^2} + A \cos(2\pi \bar{n} r) \left(\frac{1}{r}\right)^{2g_{\text{eff}}}, \quad (4)$$

where A is a constant, and \bar{n} is the mean occupation per lattice site. Using these values we computed approximate reflection coefficients, which are plotted in Fig. 2(d). They

show very good quantitative agreement with R in our simulations for $V_R > 0$, and only small deviations for $V_R < 0$, especially for initial density excitations containing approximately one particle. This agreement is better than might be expected, and demonstrates both the generality of LL theory in its applicability to low energy states of 1D systems and its continued applicability when we introduce by hand the boundary in the interaction strength. For comparison we have also computed g_{eff} based on the approximate analytical expression.

We now investigate the time propagation of the excitations when V_i varies linearly over M_b sites, which provides a more realistic treatment of barriers that might be created in a real experiment. An example shaded plot of the atom density at each site for an excitation exhibiting Andreev-like reflection is shown in Fig. 3(a). The extended length barrier spreads the resulting reflected and transmitted excitations in space [cf. Fig. 2(b)]. However, the total amplitude of the reflected wave packet is actually increased, as is seen in Fig. 3(b), where we plot the reflection coefficient R as a function of M_b for different amplitudes of the incident excitation. This brings the reflection coefficients closer to the values obtained from the effective LL parameters. The finite-width barrier also smooths the local density minima or maxima that appear at the boundary in the ground state [see Fig. 3(a)].

To provide a simpler experimental implementation, we consider the dynamics of excitations at an interaction boundary in the Bose-Hubbard model. In the perturbation theory limit, it follows from $|J/U| \ll 1$ that $|V_{i,\text{eff}}| \ll J$, and thus the amplitude of all reflections will be extremely small. However, with numerical simulations we can treat the system beyond the limit in which perturbation theory is valid. In Fig. 4(a) we show results in which a density excitation (created as for the extended Hubbard model)

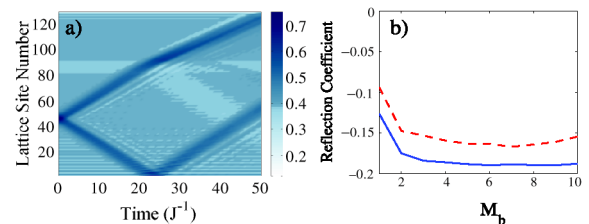


FIG. 3 (color online). Reflections of a density excitation ($\varepsilon_0 = 2J$, $x_0 = 45$, $x_b = 90 - M_b$) from a thick boundary with V_i varying from $V_L = 0$ to $V_R = -J$ linearly over M_b lattice sites. (a) Shaded density plot showing reflection of an initial density excitation with $\sigma = 3$ from a boundary with $M_b = 10$, showing the considerably broader reflected wave produced by the thick boundary. (b) Reflection coefficient as a function of barrier thickness M_b (measurement sites 55–85), showing an increase in the amplitude of the negative density reflection as the barrier is increased, for initial wave packets with $\sigma = 3$ (solid line) and $\sigma = 2$ (dashed line). The amplitude is also slightly larger for the narrower initial wave packet. $\varepsilon_0(t = 0) = 2J$.

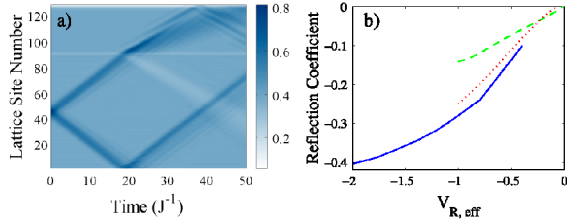


FIG. 4 (color online). Realization of Andreev reflections within the Bose-Hubbard model. (a) Shaded density plot showing an Andreev-like reflection from a boundary at $X_b = 90$, with $U_L = 10J$ and $U_R = J$. (b) Reflection coefficients for different U_R as a function of $V_{R,\text{eff}}$ for the Bose-Hubbard model (solid line). These are compared with results from the extended Hubbard model (dashed line) and estimated parameters from LL theory (dotted line) computed as in Fig. 2. Parameters used: $\varepsilon_0 = 2J$, $\sigma = 3$, $x_0 = 45$, $X_b = 90$, $M_b = 1$, $U_L = 10J$, measurement sites 55–85.

propagates across an interaction boundary at x_b with $U_{i < x_b} = 10J$ and $U_{i \geq x_b} = J$, and see clearly a reflected hole excitation. Reflection coefficients as a function of $V_{L,\text{eff}} = 1/U_{i > x_b}$ are plotted in Fig. 4(b), and compared with results for the extended Hubbard model with $V_{i > x_b} = V_{i,\text{eff}}$. Effects that go beyond the validity of perturbation theory actually yield a slight increase in the amplitude of Andreev-like reflections and bring these results close to those predicted using the estimated Luttinger parameters that were plotted in Fig. 2(d). In addition, we can use values of $U \sim J$, where $|V_{\text{eff}}/J| > 1$ without adverse boundary effects that prevent us from obtaining a smooth background density near the interaction boundary. Thus, it is possible to observe even larger amplitude Andreev-like reflections in the Bose-Hubbard model than in the extended Hubbard model.

The values of U/J used in the simulations are readily generated in homogenous systems [8], and a varying U_i could be engineered simply in several ways. For example, lasers focused on one side of the system could couple the atoms off resonantly from their internal state $|\alpha\rangle$ to an additional internal state $|\beta\rangle$. Using a Feshbach resonance [12], the interaction $U_{\alpha\alpha}$ between two atoms in the state α can be made much larger than that for atoms either in different states, $U_{\alpha\beta}$, or both in the state $|\beta\rangle$, $U_{\beta\beta}$. Thus, the admixture of the state β will reduce the on-site interaction strength in the region where the internal state of the atoms is $|\psi\rangle = a_1|\alpha\rangle + a_2|\beta\rangle$, where a_1 and a_2 are complex coefficients. Such a laser coupling could be focused so that the coupling varies on a length scale of $\lesssim 5 \mu\text{m}$, or approximately 10 lattice sites. Similarly, the initial density excitation could be prepared using a laser focused over ~ 10 lattice sites.

We have shown how wave packet dynamics of Andreev-like reflections in Hubbard models closely matches the

behavior expected from LL physics, and how these reflections could be observed time dependently with cold atoms in optical lattices. This could be extended to multispecies models and to other geometries such as Y junctions [13].

We thank U. Schollwöck, A. Kantian, N. Davidson, A.M. Rey, and G. Pupillo for discussions. Work in Innsbruck was supported by Austrian FWF project I118_N16 (EuroQUAM_DQS) and SFB F15, and by the EU networks OLAQUI and SCALA. Work in Basel was supported by the Swiss NSF and the NCCR Nanoscience.

-
- [1] T. Giamarchi, *Quantum Physics in One Dimension* (Oxford University, New York, 2004).
 - [2] T. Kinoshita, T. Wenger, and D. S. Weiss, *Science* **305**, 1125 (2004); B. Paredes *et al.*, *Nature (London)* **429**, 277 (2004); T. Stöferle *et al.*, *Phys. Rev. Lett.* **92**, 130403 (2004); S. Hofferberth *et al.*, *Nature (London)* **449**, 324 (2007).
 - [3] J. Esteve *et al.*, *Phys. Rev. Lett.* **96**, 130403 (2006); A. Widera *et al.*, arXiv:0709.2094 [Phys. Rev. Lett. (to be published)]; C. D. Fertig *et al.*, *Phys. Rev. Lett.* **94**, 120403 (2005); T. Kinoshita, T. R. Wenger, and D. S. Weiss, *Nature (London)* **440**, 900 (2006).
 - [4] D. S. Petrov, G. V. Shlyapnikov, and J. T. M. Walraven, *Phys. Rev. Lett.* **85**, 3745 (2000); V. Gritsev, E. Altman, E. Demler, and A. Polkovnikov, *Nature Phys.* **2**, 705 (2006).
 - [5] C. Kollath, U. Schollwöck, and W. Zwerger, *Phys. Rev. Lett.* **95**, 176401 (2005); A. Recati *et al.*, *ibid.* **90**, 020401 (2003); L. Kecke, H. Grabert, and W. Häusler, *ibid.* **94**, 176802 (2005); A. Kleine *et al.*, *Phys. Rev. A* **77**, 013607 (2008).
 - [6] G. Vidal, *Phys. Rev. Lett.* **91**, 147902 (2003); A. J. Daley *et al.*, *J. Stat. Mech.* (2004) P04005; S. R. White and A. E. Feiguin, *Phys. Rev. Lett.* **93**, 076401 (2004); F. Verstraete, J. J. Garcia-Ripoll, and J. I. Cirac, *ibid.* **93**, 207204 (2004).
 - [7] D. L. Maslov and M. Stone, *Phys. Rev. B* **52**, R5539 (1995); V. V. Ponomarenko, *ibid.* **52**, R8666 (1995); I. Safi and H. J. Schulz, *ibid.* **52**, R17040 (1995); I. Safi and H. J. Schulz, arXiv:cond-mat/9605014.
 - [8] I. Bloch, J. Dalibard, and W. Zwerger, arXiv:0704.3011v1 [Rev. Mod. Phys. (to be published)]; D. Jaksch and P. Zoller, *Ann. Phys. (N.Y.)* **315**, 52 (2005); M. Lewenstein *et al.*, *Adv. Phys.* **56**, 243 (2007).
 - [9] F. Dolcini, B. Trauzettel, I. Safi, and H. Grabert, *Phys. Rev. B* **71**, 165309 (2005).
 - [10] A. Micheli, G. K. Brennen and P. Zoller, *Nature Phys.* **2**, 341 (2006); V. W. Scarola and S. Das Sarma, *Phys. Rev. Lett.* **95**, 033003 (2005).
 - [11] D. Gobert, C. Kollath, U. Schollwöck, and G. Schütz, *Phys. Rev. E* **71**, 036102 (2005).
 - [12] T. Köhler, K. Góral, and P. S. Julienne, *Rev. Mod. Phys.* **78**, 1311 (2006).
 - [13] A. Tokuno, M. Oshikawa, and E. Demler, arXiv:cond-mat/0703610 [Phys. Rev. Lett. (to be published)].